Helix-coil transition in homopolypeptides under stretching

M. N. Tamashiro* and P. Pincus†
Materials Research Laboratory, University of California, Santa Barbara, California 93106-5130
(Received 2 October 2000; published 26 January 2001)

We consider the effect of an external applied force on the α-helix–coil transition of a single-stranded homopolypeptide chain. An annealed scenario is assumed, where the building amino acid monomers may interconvert between random-coiled and ordered α-helical configurations. By exact evaluation of the partition function of the freely jointed chain with helix-coil internal degrees of freedom in the thermodynamic limit, we obtain the result that the stress-strain characteristic has an asymmetrical sigmoid shape with a prominent pseudoplateau. Because of the one-dimensional nature of this system, fluctuations dominate over the mean-field approximation, which incorrectly predicts a second-order phase transition.

DOI: 10.1103/PhysRevE.63.021909 PACS number(s): 87.15.Aa, 05.70.Fh, 87.15.La, 61.41.+e

Recent developments of experimental techniques enable us to manipulate individual macromolecules [1]. New force-measurement apparatuses, which include magnetic and optical tweezers, microneedles, micropipets, flexible atomic-force microscope cantilevers, and fluorescently labeled dyes in an elongational flow, have been applied to measure the forces required to deform (by stretching, shearing, or twisting) and unfold single molecules. Experiments have been carried out on several distinct systems, including DNA [2–8], the proteins titin [9–13] and tenascin [14], the polysaccharides dextran [15] and xanthan [16], the water-soluble polymers PEG [17] (polyethylene glycol) and PVA [18] (polyvinyl alcohol), single chromatin fibers [19], and small peptide chains [20]. Due to the rich structural complexity and wide diversity of binding mechanisms involved, the theoretical interpretation of the experimental results represents a challenging task. Most of the theoretical approaches to analyzing the experimental data are based on generic polymer models of homogeneous chains stretched in their entropic regimes, like, e.g., the freely jointed [21,22] or wormlike [23,24] chain models. Since real biopolymers usually have hierarchical substructures, it is important to study the interplay between chain flexibility and structural intrachain degrees of freedom. Theoretical investigations in some specific cases, like, e.g., B/S-DNA [5,25], DNA-protein complexes [26,27], proteins [28,29], collapsed flexible globular polymers in poor solvents [30], weakly charged polyelectrolyte necklaces [31,32], polyampholytic necklaces [33], macroion-polyelectrolyte complexes [34], polysoaps [35], and homopolypeptides [36], present plateaus or pseudoplateaus, reminiscent of phase coexistence between different conformations, or abrupt stepwise behavior, related to discrete unraveling of internal structural blocks.

Beside recent experimental progress in single-molecule nanomanipulation, the α-helix–coil transition in polypeptides has been one of the well-investigated conformational transitions in biomolecules, from the experimental as well as from the theoretical point of view [37–40]. As response to variations of environmental conditions, like temperature, pH, or solvent, polypeptides may undergo dramatic configurational changes from randomly coiled forms to rodlike ordered structures associated with α helices. Their stability depends mainly on intrachain forces, e.g., dipole-dipole van der Waals interactions and the formation of hydrogen bonds between amino acid monomers along the polypeptide chain. Similar conformational transitions, like, e.g., protein folding from random denatured to compact native forms, indeed have vital biological implications. In fact, the formation of ordered α helices is ubiquitous in the secondary structure of proteins [41], which may be considered inhomogeneously charged heteropolypeptides. The particular folded conformation of a native protein is the result of the interactions of the specific sequence of amino acids that comprise the polypeptide chain [42,43]. Another example is the replication and RNA transcription of DNA, where the local disruption of the double-helix structure of the DNA is necessary in order that these fundamental genetic processes take place. Although the microscopic origins of protein folding-unfolding are more complicated than helix-coil transitions in polypeptides, the study of the latter may shed some light on the understanding of the stabilizing and destabilizing mechanisms of the ordered states that may be common to both. In view of today's facile synthesis of block copolypeptides with well-defined amino acid sequences [44] and the single-molecule manipulations described above, it is interesting to consider the effect of an external stress on the helix-coil transition of a polypeptide chain. This analysis allows us to extract structural information from single-molecule force measurements and test theoretical predictions on the stress-induced α-helix–coil transition of polypeptides.

We consider a single-stranded homopolypeptide chain that may undergo an α-helix–coil transition. The chain is comprised of N amino acid monomers (residues), which are linked to its neighbors by covalent peptide bonds and may interconvert between coiled (c) and α-helical (h) conformations. For each monomer $i=1,\ldots,N$ is assigned a state variable μ_i, which takes the value $\mu_i=0$ for the coiled or $\mu_i=1$ for the helical state. Therefore, there are altogether 2^N distinct allowed conformational states for the chain. The unstretched-chain equilibrium properties are the subject of a vast literature [37–40]. Although in a real polypeptide chain the hydrogen bonds are formed between the NH (amide)

*Electronic address: mtamash@mrl.ucsb.edu
†Electronic address: fyl@mrl.ucsb.edu

group i and the CO (carboxyl) group $i+4$, we will use the simpler approach adopted by Zimm and Bragg [45], in which the hydrogen bonding takes place between two adjacent monomers. In this case, in the absence of any external forces, the partition function is constructed assigning different statistical weights for the four possible configurations of a given residue relative to its predecessor. These configurations are *cc*, *hc*, *ch*, and *hh*, whose corresponding weights are 1, 1, σs, and s, respectively. The nucleation constant σ and the helical propagation parameter s govern the behavior of the system. They represent the Boltzmann weight $\sigma = e^{-2\Delta w/k_B T}$ for the formation of a helical sequence and the statistical weight $s = e^{-\Delta f/k_B T}$ for a residue in a helical state (relative to the coiled). $2\Delta w$ represents the interfacial energy associated with a helical domain and Δf corresponds to the change in the free energy due to the intrachain hydrogen bonding and the loss of configurational entropy. The partition function can be readily obtained using the matrix formulation of Zimm and Bragg [45],

$$Z_0 = \sum_{\{\mu_i\}} \prod_{i=1}^{N} \sigma^{(1-\mu_i)\mu_{i+1}} s^{\mu_{i+1}} = \mathrm{Tr}\, \mathbb{M}^N = \lambda_0^N + \lambda_1^N, \quad (1)$$

which is written in terms of the transfer matrix $\mathbb{M} = \begin{pmatrix} 1 & \sigma s \\ 1 & s \end{pmatrix}$ of elements $M_{\mu_i \mu_{i+1}} = \sigma^{(1-\mu_i)\mu_{i+1}} s^{\mu_{i+1}}$ and eigenvalues

$$\lambda_{0,1} = \tfrac{1}{2}[1 + s \pm \sqrt{(1-s)^2 + 4\sigma s}]. \quad (2)$$

In order to identify the partition function with the trace of $\mathbb{M}^N$, we assumed periodic boundary conditions, $\mu_{N+1} \equiv \mu_1$. Any errors incurred by chain-end effects will vanish in the limit of long chains. Since the system is one dimensional and the interactions are short ranged, even at the infinite-chain limit ($N \to \infty$) a true thermodynamical phase transition occurs only for $\sigma = 0$, when the transfer matrix is not positive definite and the Perron-Frobenius theorem does not apply [46]. The sharpness of the crossover region is controlled by σ, whereas s is related to the temperature. However, there have been indications that the polypeptide-chain adsorption to an interface [47] or the introduction of long-ranged Coulomb interactions [48,49] may promote the helix-coil transition into a true critical phenomenon, even for finite σ.

The effect of an external applied force on the helix-coil transition is analyzed using a simple model first introduced by Nagai [50]. In fact, a mean-field treatment of this model was previously performed by Buhot and Halperin [36]. As discussed in Appendix B, the present work represents an extension of their calculation, in which the partition function is evaluated exactly and fluctuations are automatically taken into account. Each uninterrupted helical sequence containing n residues is replaced by a rod of length $n l_{\mathrm{helix}}$, where l_{helix} is the projection along the α-helix axis of the distance per residue. On the other hand, the coiled regions are replaced by a freely jointed chain [21,22] with segments of bond length l_{coil}. The ratio between the helical and coiled-bond lengths, $\gamma = l_{\mathrm{helix}}/l_{\mathrm{coil}}$, is restricted to the range 0 to 1. The effect of the external applied force $\mathbf{F}$ is taken into account by adding to the Hamiltonian an elastic contribution $-\mathbf{F}\cdot(\mathbf{r}_N - \mathbf{r}_0) = -\mathbf{F}\cdot\sum_{i=1}^{N}(\mathbf{r}_i - \mathbf{r}_{i-1}) = -F\sum_{i=1}^{N} l_i \cos\vartheta_i$, where $\mathbf{r}_{i-1}$ represents the three-dimensional position vector of the starting point of the ith residue [or the end of the $(i-1)$th residue], $l_i = l_{\mathrm{coil}}$ for the coiled state ($\mu_i = 0$), $l_i = l_{\mathrm{helix}}$ for the helical state ($\mu_i = 1$), and ϑ_i is the angle between the ith residue and the z axis, the direction of the stretching force $\mathbf{F}$. Monomer units in a coiled conformation are free to rotate independently over all angles, while a residue in a helical block is restricted to coherently rotate with the other segments that compose the same helical region. However, we will assume that there are no correlations between distinct helical sections. Orientational correlations between successive helical sequences may be relevant in the presence of short coiled sequences. Under these conditions, the partition function in the presence of external forces can be formally written as

$$Z_F = \prod_{k=1}^{N}\left[\frac{1}{4\pi}\int_0^{2\pi} d\phi_k \int_{-1}^{1} d\xi_k\right] \times \sum_{\{\mu_i\}} \prod_{i=1}^{N} \Xi_i(\Omega_i, \Omega_{i+1})\, \sigma^{(1-\mu_i)\mu_{i+1}} s^{\mu_{i+1}}, \quad (3)$$

where $\Omega_i = \{\phi_i, \xi_i = \cos\vartheta_i\}$, and the force-dependent function $\Xi_i(\Omega_i, \Omega_{i+1}) = e^{\varphi\xi_i}(1-\mu_i) + e^{\gamma\varphi\xi_i}\mu_i(1-\mu_{i+1}) + 4\pi e^{\gamma\varphi\xi_i}\delta(\Omega_i - \Omega_{i+1})\mu_i\mu_{i+1}$, with δ the Dirac delta function. $\varphi = F l_{\mathrm{coil}}/k_B T$, and $\gamma\varphi = F l_{\mathrm{helix}}/k_B T$ are the dimensionless elastic energies associated with the coiled and helical residues, respectively. Although it is possible to write a formal expression of the partition function in terms of a multidimensional integral of a product of transfer matrices, such a form would be useless due to the coupling introduced by the Dirac δ functions. Therefore we must resort to a combinatorial approach for the evaluation of Z_F. In addition to the unstretched-chain statistical weights, we have an elastic factor $S(\varphi) \equiv (1/4\pi)\int_0^{2\pi} d\phi \int_{-1}^{1} d\xi\, e^{\varphi\xi} = \sinh\varphi/\varphi$ for each coiled residue and an $S(n\gamma\varphi)$ factor for each uninterrupted helical sequence containing n residues. There are many degeneracies in the 2^N distinct terms of the partition function, which can be rewritten as a sum,

$$Z_F = s^N S(N\gamma\varphi) + S^N(\varphi)\sum_{\mathbf{k}} C_{\mathbf{k}} \prod_{n=1}^{N-1}\left[\frac{\sigma s^n S(n\gamma\varphi)}{S^n(\varphi)}\right]^{k_n}. \quad (4)$$

The first term of Eq. (4) represents the statistical weight of the pure-helix configuration, while the weight corresponding to the fully coiled state is given by the term $\mathbf{k} = \mathbf{0}$ of the sum. The sum over $\mathbf{k} \equiv (k_1, \ldots, k_{N-1})$ is restricted to all nonnegative integer values of k_n ($n = 1, \ldots, N-1$) subject to the constraint

$$\sum_{n=1}^{N-1} (n+1)k_n \leqslant N, \quad (5)$$

and

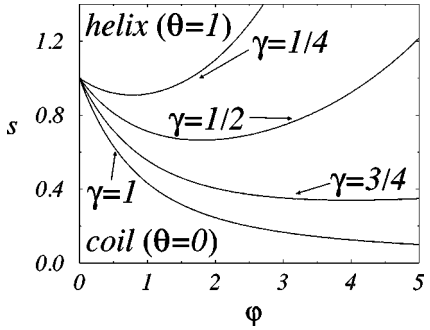

FIG. 1. Phase diagram on the $s\times\varphi$ plane for the fully cooperative case ($\sigma=0$) in the infinite-chain limit ($N\to\infty$) and for several values of the ratio between the helical and coiled bond lengths, γ. Above the continuous lines, which represent the critical value given by Eq. (9), we have an ordered rodlike α-helix configuration, whereas for smaller values of s the chain is in a coiled conformation.

$$C_{\mathbf{k}}=\frac{N\left(N-1-\sum_{n=1}^{N-1}nk_n\right)!}{\left(N-\sum_{n=1}^{N-1}(n+1)k_n\right)!\prod_{n=1}^{N-1}k_n!} \tag{6}$$

is the number of distinct possible configurations containing k_n uninterrupted helical regions of size $n, n=1,\ldots,N-1$. In fact, the constraint (5) is automatically taken into account by the combinatorial factor $C_{\mathbf{k}}$, because $1/[N-\Sigma_{n=1}^{N-1}(n+1)k_n]!=0$ for $\Sigma_{n=1}^{N-1}(n+1)k_n>N$.

For the fully cooperative case ($\sigma=0$), only the two pure-state terms of the partition function survive, $Z_F(\sigma=0)=s^N S(N\gamma\varphi)+S^N(\varphi)$. Two physical quantities may be obtained by differentiation of the logarithm of the partition function, namely, the fraction of monomers in helical regions, $\theta_N=(1/N)\Sigma_{i=1}^{N}\langle\mu_i\rangle=(1/N)d(\ln Z_F)/d(\ln s)$, where $\langle\cdots\rangle$ denotes an average in the stress ensemble defined by Z_F, and the normalized dimensionless average length of the chain along the force direction, $r=(1/Nl_{\mathrm{coil}})\Sigma_{i=1}^{N}\langle l_i\cos\vartheta_i\rangle=(1/N)d(\ln Z_F)/d\varphi$, which is limited to the range 0 to 1. In the limit of long chains, $N\to\infty$, the transition becomes discontinuous,

$$\theta=\lim_{N\to\infty}\theta_N=\lim_{N\to\infty}\left[1+\frac{S^N(\varphi)}{s^N S(N\gamma\varphi)}\right]^{-1}=\begin{cases}0 & \text{for } s<s_{\mathrm{crit}}\\ 1 & \text{for } s>s_{\mathrm{crit}},\end{cases} \tag{7}$$

$$r=\lim_{N\to\infty}[(1-\theta_N)\mathcal{L}(\varphi)+\theta_N\gamma\mathcal{L}(N\gamma\varphi)]=\begin{cases}\mathcal{L}(\varphi) & \text{for } s<s_{\mathrm{crit}}\\ \gamma & \text{for } s>s_{\mathrm{crit}},\end{cases} \tag{8}$$

where $\mathcal{L}(\varphi)=\coth\varphi-1/\varphi$ is the Langevin function, taking place at the critical value

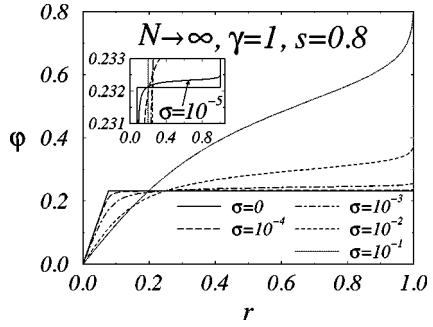

FIG. 2. Force-extension profiles in the infinite-chain limit ($N\to\infty$), for $\gamma=1$, $s=0.8$, and several values of the cooperativity parameter σ. The plateau obtained resembles early experimental measurements of the melting of an ideal homogeneous fibril consisting of a parallel bundle of polypeptide chains [51]. To allow a better view of the crossover region for very small values of σ, the inset displays a magnification of the plateau neighborhood. Notice that the finite-σ force-extension profiles do not cross the $\sigma=0$ plateau at its middle point, in contrast to a previous calculation by Buhot and Halperin [36] for the case of an external imposed strain—see the discussion in Appendix B.

$$s_{\mathrm{crit}}=e^{-\gamma\varphi}S(\varphi). \tag{9}$$

For finite values of N, the crossover region has a finite width, which is broader for smaller values of N. In Fig. 1 the $s\times\varphi$ phase diagram for the fully cooperative case ($\sigma=0$) in the infinite-chain limit $N\to\infty$ is presented for some values of γ. For any value of $\gamma<1$, we obtain two transitions for a certain range of the parameter s. Initially we observe a stress-induced stiffening of the chain, because the alignment of coiled segments along the force direction favors the formation of the ordered α helix. The second transition, occurring at strong deformations, involves the rupture of the stabilizing hydrogen bonds of the α helix. Only for $\gamma=1$ is the critical value (9) a monotonically decreasing function of the stress φ, and the second hydrogen-bond breaking transition does not occur. The fully cooperative $\sigma=0$ force-elongation profile, given by Eq. (8), is presented in Figs. 2 and 3, together with the profiles for finite σ. It is worth mentioning that similar

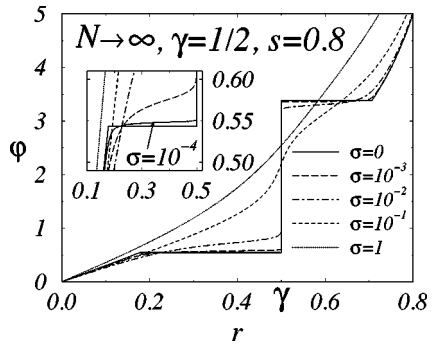

FIG. 3. Force-extension profiles in the infinite-chain limit ($N\to\infty$), for $\gamma=1/2$, $s=0.8$, and several values of the cooperativity parameter σ. To allow a better view of the crossover region for very small values of σ, the inset displays a magnification of the plateau vicinity, showing that the finite-σ sigmoid profiles are not symmetrical about the crossing point (r_p,φ_p).

force-length behavior has been observed in early experiments on the stretching of a parallel bundle of polypeptide chains [51].

For the finite cooperative case ($\sigma \neq 0$), a closed expression for the partition function can be obtained only in the infinite-chain limit ($N \to \infty$)—see the derivation in Appendix A. The equations of state, the Gibbs free energy per residue, $g = -k_B T \lim_{N\to\infty}(1/N)\ln Z_F$, and the force-extension relation are written in terms of the variables $x \equiv 1-\theta$ and $y \equiv 1-\theta-\eta$, where the mean fraction of helical monomer units following coiled segments is $\eta \equiv \lim_{N\to\infty}(1/N)\Sigma_{i=1}^{N}\langle(1-\mu_i)\mu_{i+1}\rangle = \lim_{N\to\infty}(1/N)d(\ln Z_F)/d(\ln\sigma)$,

$$x = X(x,y,\varphi) = 1 - \frac{\sigma x y^2 s S(\varphi) S(\gamma\varphi)}{[xS(\varphi) - yse^{\gamma\varphi}][xS(\varphi) - yse^{-\gamma\varphi}]}, \tag{10}$$

$$y = Y(x,y,\varphi) = x + \frac{\sigma y}{2\gamma\varphi}\ln\left[\frac{xS(\varphi) - yse^{\gamma\varphi}}{xS(\varphi) - yse^{-\gamma\varphi}}\right], \tag{11}$$

$$-\frac{g}{k_B T} = \begin{cases} \ln S(\varphi) + \ln\dfrac{x}{y} & \text{for } s < s_{\rm crit}\dfrac{x}{y} \\ \gamma\varphi + \ln s & \text{for } s > s_{\rm crit}\dfrac{x}{y}, \end{cases} \tag{12}$$

$$r = \begin{cases} x\mathcal{L}(\varphi) + \dfrac{y-x}{\varphi} + \dfrac{1}{2\varphi}\left\{\dfrac{[x^2S^2(\varphi) - y^2s^2](1-x)}{xysS(\varphi)S(\gamma\varphi)} - \sigma y\right\} & \text{for } s < s_{\rm crit}\dfrac{x}{y} \\ \gamma \quad \text{for } s > s_{\rm crit}\dfrac{x}{y}, \end{cases} \tag{13}$$

where $s_{\rm crit}$ is the unstretched critical propagation parameter, given by Eq. (9).

In Figs. 2 and 3 we present some typical force-extension profiles for finite values of the nucleation parameter σ. Note the steep increase of the force at $r = \gamma$ related to the stiffening of the chain and the asymmetrical sigmoid shape in the vicinity of the $\sigma = 0$ plateau. In Appendix B these exact results are compared with a mean-field approximation for the partition function [36], which incorrectly leads to a (continuous) second-order phase transition for finite σ.

The asymptotic behavior about $\sigma = 0$ is given by a slowly convergent series, because the expansion parameter ϵ (defined below) has a logarithmic dependence on σ. In leading order, we may show that the plateau crossings (for both low- and high-force transitions when $0 < \gamma < 1$) occur at

$$\lim_{\sigma\to 0} x_p \approx 1 + \psi(\epsilon), \tag{14}$$

$$\lim_{\sigma\to 0} y_p \approx 1 + \psi(\epsilon) + \frac{\sigma}{2\epsilon\gamma\varphi_p}, \tag{15}$$

$$\lim_{\sigma\to 0} r_p \approx \mathcal{L}(\varphi_p) + [\mathcal{L}(\varphi_p) - \gamma]\psi(\epsilon) + \frac{\sigma}{2\epsilon\gamma\varphi_p^2}, \tag{16}$$

$$\epsilon^{-1} = -W\left[\frac{2\gamma\varphi_p(1 - e^{-2\gamma\varphi_p})}{e\sigma}\right], \tag{17}$$

$$\psi(\epsilon) = \frac{1 - 2\epsilon - \sqrt{1-4\epsilon}}{2\epsilon} = \epsilon + 2\epsilon^2 + 5\epsilon^3 + 14\epsilon^4 + 42\epsilon^5 + 132\epsilon^6 + O(\epsilon^7), \tag{18}$$

where the stress value at the $\sigma = 0$ plateau, φ_p, is given by the solution of Eq. (9) for a given s, and $W(z)$ is the principal solution of the Lambert W function [52,53], which is defined to be the multivalued inverse of the transcendental equation $z = We^W$. Notice that, as we approach the fully cooperative limit ($\sigma \to 0$), we obtain $\epsilon \to 0$, $\sigma/\epsilon \to 0$ and the plateau crossing r_p tends to the edge value $\mathcal{L}(\varphi_p)$ corresponding to the pure coiled-state length, giving rise to a highly asymmetric sigmoid form for small σ.

We may expand the force-extension relation in the vicinity of the $\sigma = 0$ plateau to obtain the asymptotic linear elasticity law

$$\varphi = \varphi_p + (r - r_p)\left.\frac{d\varphi}{dr}\right|_{\varphi=\varphi_p} + O[(r - r_p)^2], \tag{19}$$

where the slope, in leading order about $\sigma \to 0$, is given by

$$\lim_{\sigma\to 0}\left.\frac{d\varphi}{dr}\right|_{\varphi=\varphi_p}=\frac{\sigma\Delta_1}{\epsilon^2\Delta_2+\sigma\Delta_3}, \tag{20}$$

with coefficients $\Delta_1=[1+\psi(\epsilon)]^5\{1-\epsilon[1+\psi(\epsilon)]\}^2$, $\Delta_2=2\gamma\varphi_p[1+\psi(\epsilon)]^8[\mathcal{L}(\varphi_p)-\gamma]^2$, and $\Delta_3=1-2\mathcal{L}(\varphi_p)/\varphi_p-\mathcal{L}^2(\varphi_p)$. Since $\sigma/\epsilon^2\to 0$ as $\sigma\to 0$, the asymptotic slope (20) vanishes logarithmically as $\sigma W^2(1/\sigma)\approx\sigma[\ln\sigma+\ln|\ln\sigma|]^2$, which is distinct from the mean-field power-law dependence $\sigma^{1/2}$ given by Eq. (B11).

In Appendix B we show that a previous calculation by Buhot and Halperin [36] corresponds indeed to a mean-field approximation for the partition function. However, we should mention that a mean-field approach is inappropriate for this system, because it is not possible to perform a perturbation theory about the mean-field solution. Due to the low dimensionality of the system, this is not at all surprising. This impossibility is due to the fact that the higher-order moments of the block-size distribution $\langle k_n^\nu\rangle$ scale like $N^{\nu-1}$. Indeed, in the infinite-chain limit, the ratio

$$\begin{aligned}\lim_{N\to\infty}\frac{1}{N^{\nu-1}}\langle k_n^\nu\rangle&=\lim_{N\to\infty}\frac{1}{N^\nu}\sum_{n=1}^{N-1}k_n^\nu\\&=\left[\frac{\sigma(1-\theta-\eta)}{2\gamma\varphi}\right]^\nu\sum_{j=0}^{\nu}(-1)^j\binom{\nu}{j}\\&\quad\times\mathrm{Li}_\nu\left\{\left[\frac{(1-\theta-\eta)se^{\gamma\varphi}}{(1-\theta)S(\varphi)}\right]^\nu e^{-2j\gamma\varphi}\right\}\end{aligned} \tag{21}$$

is finite and can be expressed in terms of the νth polylogarithmic function [54] $\mathrm{Li}_\nu(z)=\Sigma_{j=1}^\infty z^j/j^\nu$.

In summary, we have provided an exact treatment of the stress-induced α-helix–coil transition in homopolypeptides, in which the elastic degrees of freedom are analyzed in the framework of the freely jointed chain model. This statistical-mechanical standpoint, besides being straightforward, has the advantage of enabling an accurate control over the approximations. The force-extension profiles obtained are qualitatively distinct from elasticity laws derived in the mean-field approximation [36]—see the discussion in Appendix B. In particular, the sigmoid form in the crossover region has a highly asymmetric form and its asymptotic slope vanishes logarithmically, proportional to $\sigma[\ln\sigma+\ln|\ln\sigma|]^2$, in contrast to the mean-field power-law prediction proportional to $\sigma^{1/2}$. Also, the mean-field approach predicts a second-order phase transition, which is prohibited for this one-dimensional system for finite σ. Furthermore, we also showed that it is not possible to develop a perturbation theory about the mean-field solution, because fluctuations play a fundamental role and cannot be disregarded.

The authors acknowledge fruitful discussions with Arnaud Buhot and Avi Halperin. M.N.T. acknowledges the financial support of the Brazilian agency CNPq, Conselho Nacional de Desenvolvimento Científico e Tecnológico. This research was also partially supported by the MRL Program of the National Science Foundation under Grant Nos. DMR-96-32716 and DMR-96-24091.

APPENDIX A: EXACT PARTITION FUNCTION IN THE INFINITE-CHAIN LIMIT ($N\to\infty$)

We want to maximize the general term $z_{\mathbf{k}}$ of the partition function (4), $Z_F=s^N S(N\gamma\varphi)+\Sigma_{\mathbf{k}}z_{\mathbf{k}}$, or more conveniently its logarithm,

$$\begin{aligned}\lim_{N\to\infty}\ln z_{\mathbf{k}}&=N\ln S(\varphi)+1+\ln N\\&\quad+\left(N-1-\sum_{n=1}^{N-1}nk_N\right)\ln\left(N-1-\sum_{n=1}^{N-1}nk_n\right)\\&\quad-\left[N-\sum_{n=1}^{N-1}(n+1)k_n\right]\ln\left[N-\sum_{n=1}^{N-1}(n+1)k_n\right]\\&\quad-\sum_{n=1}^{N-1}k_n\ln k_n+\sum_{n=1}^{N-1}k_n\ln\left[\frac{\sigma s^n S(n\gamma\varphi)}{S^n(\varphi)}\right],\end{aligned} \tag{A1}$$

where the Stirling approximation $\ln z!\approx z\ln z-z$ was employed to obtain Eq. (A1). The stationary-point equations $\partial\ln z_{\mathbf{k}}/\partial k_n=0$ yield the distribution

$$k_n=\frac{\left(N-\sum_{n=1}^{N-1}(n+1)k_n\right)^{n+1}\sigma s^n S(n\gamma\varphi)}{\left(N-1-\sum_{n=1}^{N-1}nk_n\right)^n S^n(\varphi)}, \tag{A2}$$

which, in turn, leads to the self-consistent equations for the intensive self-averaged variables,

$$\theta\equiv\langle nk_n\rangle=\lim_{N\to\infty}\frac{1}{N}\sum_{n=1}^{N-1}nk_n=\lim_{N\to\infty}\frac{1}{N}\frac{d(\ln Z_F)}{d(\ln s)}=\frac{\sigma(1-\theta)(1-\theta-\eta)^2sS(\varphi)S(\gamma\varphi)}{[(1-\theta)S(\varphi)-(1-\theta-\eta)se^{\gamma\varphi}][(1-\theta)S(\varphi)-(1-\theta-\eta)se^{-\gamma\varphi}]}, \tag{A3}$$

$$\eta\equiv\langle k_n\rangle=\lim_{N\to\infty}\frac{1}{N}\sum_{n=1}^{N-1}k_n=\lim_{N\to\infty}\frac{1}{N}\frac{d(\ln Z_F)}{d(\ln\sigma)}=\frac{\sigma(1-\theta-\eta)}{2\gamma\varphi}\ln\left[\frac{(1-\theta)S(\varphi)-(1-\theta-\eta)se^{-\gamma\varphi}}{(1-\theta)S(\varphi)-(1-\theta-\eta)se^{\gamma\varphi}}\right]. \tag{A4}$$

In the unstretched-chain limit ($\varphi \to 0$), we regain, as expected, the unperturbed-chain Zimm-Bragg results [45] $\theta_0 = (\lambda_0 - 1)/(2\lambda_0 - 1 - s)$, $\eta_0 = (\lambda_0 - 1)(\lambda_0 - s)/[\lambda_0(2\lambda_0 - 1 - s)]$, $\lambda_0 = (1-\theta_0)/(1-\theta_0-\eta_0)$, where λ_0 is the largest eigenvalue of the unstretched-chain transfer matrix $\mathbb{M}$, given by Eq. (2).

To perform the numerical calculations for the stretched chain ($\varphi \neq 0$), it is convenient to introduce the variables $x \equiv 1-\theta$ and $y \equiv 1-\theta-\eta$, in terms of which the self-consistent equations and the Gibbs free energy per residue, $g = -\lim_{N\to\infty}(k_B T/N)\ln Z_F$, can be rewritten as Eqs. (10)–(12). The calculation of the average chain length along the force direction, $r = -(1/k_B T)dg/d\varphi|_{s,\sigma} = \mathcal{L}(\varphi) + (1/x)dx/d\varphi - (1/y)dy/d\varphi$ for $s < s_{\rm crit}x/y$, or $r = \gamma$ for $s > s_{\rm crit}x/y$, requires the derivatives of the parametric forms, $dx/d\varphi = [\partial X/\partial\varphi + \partial(X,Y)/\partial(y,\varphi)]/\Delta$, $dy/d\varphi = [\partial Y/\partial\varphi - \partial(X,Y)/\partial(x,\varphi)]/\Delta$, $\Delta = 1 - \partial X/\partial x - \partial Y/\partial y + \partial(X,Y)/\partial(x,y)$. After tedious and lengthy algebraic manipulations, we are led to the force-extension relation (13).

APPENDIX B: MEAN-FIELD APPROXIMATION FOR THE PARTITION FUNCTION

We now show that the approach followed by Buhot and Halperin [36] corresponds indeed to a mean-field approximation for the partition function. Two contributions to the general term $z_{\mathbf{k}}$ of the partition function (A1) can not be written in terms of the intensive variables θ and η. In a mean-field approach, they are approximated by

$$\sum_{n=1}^{N-1} k_n \ln k_n \to N\eta \ln(N\eta), \tag{B1}$$

$$\sum_{n=1}^{N-1} k_n \ln S(n\gamma\varphi) \to N\eta \ln S\left(\frac{\theta\gamma\varphi}{\varphi}\right). \tag{B2}$$

Note that, by assuming a mean-field approximation for the size of the helical blocks, we need to add to the entropic term a contribution $(1/N)\ln(\frac{\theta N}{\eta N})$ to account for their polydispersity. The mean-field Gibbs free energy per monomer, $\tilde{g}(\varphi) = u - Ts_{\rm mix} + g_{\rm elast}(\varphi)$, is split into three terms,

$$\frac{u}{k_B T} = -\eta \ln\sigma - \theta \ln s, \tag{B3}$$

$$-\frac{s_{\rm mix}}{k_B} = (\theta-\eta)\ln\frac{\theta-\eta}{\theta} + \eta\ln\frac{\eta}{\theta} + \eta\ln\frac{\eta}{1-\theta} + (1-\theta-\eta)\ln\frac{1-\theta-\eta}{1-\theta}, \tag{B4}$$

$$\frac{g_{\rm elast}}{k_B T} = -(1-\theta)\ln S(\varphi) - \eta \ln S\left(\frac{\theta\gamma\varphi}{\eta}\right), \tag{B5}$$

where $u - Ts_{\rm mix}$ corresponds to the unstretched-chain free energy (u is the internal energy and $s_{\rm mix}$ is the mixing entropy) and $g_{\rm elast}(\varphi)$ represents the elastic free energy in the fixed-force (stress) ensemble. Minimization of the mean-field Gibbs free energy $\tilde{g}$ with respect to θ and η leads to the mean-field equations of state,

$$(1-\theta)(\theta-\eta)S(\varphi) = \theta s(1-\theta-\eta)\exp[\gamma\varphi\mathcal{L}(\theta\gamma\varphi/\eta)], \tag{B6}$$

$$\eta^2 \exp[(\theta\gamma\varphi/\eta)\mathcal{L}(\theta\gamma\varphi/\eta)] = \sigma(\theta-\eta)(1-\theta-\eta)S(\theta\gamma\varphi/\eta). \tag{B7}$$

In fact, the stress-ensemble (fixed-force) Gibbs elastic free energy $g_{\rm elast}$ corresponds to the Legendre transform of the strain-ensemble (fixed-length) Helmholtz elastic free energy $f_{\rm elast}$ considered by Buhot and Halperin [36], $f_{\rm elast}(r) = g_{\rm elast}[\varphi(r)] + k_B T r\varphi(r)$. However, because the elasticity law $r = -(1/k_B T)d\tilde{g}/d\varphi|_{s,\sigma} = -(1/k_B T)\partial g_{\rm elast}/\partial\varphi = (1-\theta)\mathcal{L}(\varphi) + \theta\gamma\mathcal{L}(\theta\gamma\varphi/\eta)$ cannot, in general, be analytically inverted to give $\varphi = \varphi(r)$, it is not possible to perform an exact analysis of the mean-field equations in the strain ensemble. In particular, we will show later that, contrary to Buhot and Halperin's calculations, the mean-field force-extension profiles do not have an inflection point at the middle point of the plateau. At this point we should remark that, although Buhot and Halperin obtained their plateau within the $s_{\rm mix} = 0$ approximation, this assumption becomes *exact* in the $\sigma \to 0$ limit, as can be seen by taking this limit in the mean-field equations of state. Therefore, the $s_{\rm mix} = 0$ plateau obtained by Buhot and Halperin, apart from the weak-force expansion, corresponds to the exact $\sigma = 0$ plateau. In particular, their plateau force $\tilde{\varphi}_p \approx 3 - 3\sqrt{1 + \frac{2}{3}\ln s}$ can be obtained by a second-order expansion of the critical propagation parameter s in the fully cooperative ($\sigma \to 0$) limit, Eq. (9).

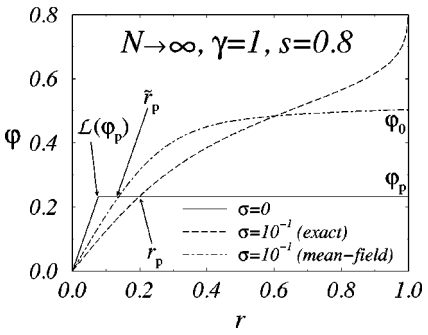

FIG. 4. Comparison between the exact and the mean-field force-extension profiles in the infinite-chain limit ($N \to \infty$), for $\gamma = 1$, $s = 0.8$, and $\sigma = 10^{-1}$. We chose a large value of σ to allow a better comparison between the two approaches; the same features are present for very small values of σ. We indicated in the figure the exact ($r = r_p$) and the mean-field ($r = \tilde{r}_p$) plateau crossings, the asymptotic $\sigma \to 0$ crossing value $\mathcal{L}(\varphi_p)$, the plateau force φ_p, and the mean-field critical force φ_0. The mean-field approximation predicts a second-order phase transition at $\varphi = \varphi_0$ between a partially and a pure helical state. The partition-function exact treatment leads to a smooth crossover between these two states and there is no true thermodynamical phase transition. The smooth crossover is related to the steep increase in the force close to $r = \gamma$.

Unlike the strain ensemble, in the stress ensemble it is possible to perform an exact analysis of the mean-field equations. In particular, one may show that the crossings with the $\sigma=0$ plateaus occur at

$$\lim_{\sigma\to 0}\theta_p \approx \frac{\sqrt{\tilde{\epsilon}}}{2}, \tag{B8}$$

$$\lim_{\sigma\to 0}\eta_p \approx \frac{\tilde{\epsilon}}{2}, \tag{B9}$$

$$\lim_{\sigma\to 0}\tilde{r}_p \approx \mathcal{L}(\varphi_p)+[\gamma-\mathcal{L}(\varphi_p)]\frac{\sqrt{\tilde{\epsilon}}}{2}, \tag{B10}$$

where the mean-field expansion parameter $\tilde{\epsilon}\equiv e\sigma/(\gamma\varphi_p)$. An analogous asymptotic linear elasticity law like (19) can be obtained at the mean-field level, replacing r_p by $\tilde{r}_p$, where the mean-field slope, in leading order about $\sigma\to 0$, is given by

$$\lim_{\sigma\to 0}\left.\frac{d\varphi}{dr}\right|_{\varphi=\varphi_p} = \frac{2\sqrt{\tilde{\epsilon}}}{[\gamma-\mathcal{L}(\varphi_p)]^2}. \tag{B11}$$

This power-law dependence ($\sigma^{1/2}$) of the mean-field slope is in contrast with the logarithmically vanishing slope (20) proportional to $\sigma[\ln\sigma+\ln|\ln\sigma|]^2$.

A point overlooked by Buhot and Halperin [36] is that the mean-field approximation incorrectly predicts a (continuous) second-order phase transition for finite σ, which is prohibited for this one-dimensional system [46]. This can be seen in Fig. 4, where the mean-field and the exact partition-function profiles are compared. The mean-field force profile meets $r=\gamma$ with vanishing slope (in the $\sigma\to 0$ limit) $\lim_{\sigma\to 0} d\varphi/dr|_{\varphi=\varphi_0}\propto\sigma^2$, at a critical force φ_0 satisfying exactly (for all values of σ) the condition

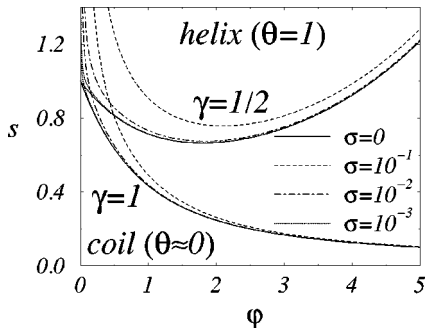

FIG. 5. Mean-field $s\times\varphi$ phase diagram in the infinite-chain limit ($N\to\infty$), for $\gamma=1$ and 1/2, $s=0.8$, and finite cooperativity ($\sigma\neq 0$). These curves, for finite σ, correspond to the boundary φ_0 of the helical region, given by Eq. (B12), and represent the loci of the (continuous) second-order phase transition. For a fixed external force φ, the transition is shifted to higher values of s.

$$s = e^{-\gamma\varphi_0}S(\varphi_0)\left(1+\frac{e\sigma}{2\gamma\varphi_0}\right). \tag{B12}$$

In the $\sigma\to 0$ limit, $\varphi_0\to\varphi_p$. A noteworthy feature is that the mean-field force-extension profile does not have an inflection point, its derivative for $r<\gamma$ being a monotonically decreasing function of the reduced length r. This is in contrast with the exact partition-function result, which predicts a steep increase in the force close to $r=\gamma$. In Fig. 5 we present the mean-field $s\times\varphi$ phase diagram for finite cooperativity ($\sigma\neq 0$). For a given external force φ, the $\sigma=0$ first-order (discontinuous) transition is shifted to higher values of s and becomes second order (continuous).

[1] A. D. Mehta, M. Rief, J. A. Spudich, D. A. Smith, and R. M. Simmons, Science **283**, 1689 (1999).

[2] T. T. Perkins, S. R. Quake, D. E. Smith, and S. Chu, Science **264**, 822 (1994).

[3] T. T. Perkins, D. E. Smith, R. G. Larson, and S. Chu, Science **268**, 83 (1995).

[4] S. B. Smith, Y. Cui, and C. Bustamante, Science **271**, 795 (1996).

[5] P. Cluzel, A. Lebrun, C. Heller, R. Lavery, J.-L. Viovy, D. Chatenay, and F. Caron, Science **271**, 792 (1996).

[6] T. R. Strick, J.-F. Allemand, D. Bensimon, A. Bensimon, and V. Croquette, Science **271**, 1835 (1996).

[7] T. T. Perkins, D. E. Smith, and S. Chu, Science **276**, 2016 (1997).

[8] R. H. Austin, J. P. Brody, E. C. Cox, T. Duke, and W. Volkmuth, Phys. Today **50** (2), 32 (1997).

[9] L. Tskhovrebova, J. Trinick, J. A. Sleep, and R. M. Simmons, Nature (London) **387**, 308 (1997).

[10] M. S. Z. Kellermayer, S. B. Smith, H. L. Granzier, and C. Bustamante, Science **276**, 1112 (1997).

[11] M. Rief, M. Gautel, F. Oesterhelt, J. M. Fernandez, and H. E. Gaub, Science **276**, 1109 (1997).

[12] H. P. Erickson, Science **276**, 1090 (1997).

[13] M. B. Viani, T. E. Schäffer, G. T. Paloczi, L. I. Pietrasanta, B. L. Smith, J. B. Thompson, M. Richter, M. Rief, H. E. Gaub, K. W. Plaxco, A. N. Cleland, H. G. Hansma, and P. K. Hansma, Rev. Sci. Instrum. **70**, 4300 (1999).

[14] A. F. Oberhauser, P. E. Marszalek, H. P. Erickson, and J. M. Fernandez, Nature (London) **393**, 181 (1998).

[15] M. Rief, F. Oesterhelt, B. Heymann, and H. E. Gaub, Science **275**, 1295 (1997).

[16] H. B. Li, M. Rief, F. Oesterhelt, and H. E. Gaub, Adv. Mater. **10**, 316 (1998).

[17] F. Oesterhelt, M. Rief, and H. E. Gaub, New J. Phys. **1**, 6.1 (1999).

[18] H. B. Li, W. K. Zhang, W. Q. Xu, and X. Zhang, Macromolecules **33**, 465 (2000).

[19] Y. Cui and C. Bustamante, Proc. Natl. Acad. Sci. U.S.A. **97**, 127 (2000).

[20] M. A. Lantz, S. P. Jarvis, H. Tokumoto, T. Martynski, T. Kusumi, C. Nakamura, and J. Miyake, Chem. Phys. Lett. **315**, 61 (1999).

[21] W. Kuhn and F. Grün, Kolloid-Z. **101**, 248 (1942).
[22] S. Chandrasekhar, Rev. Mod. Phys. **15**, 1 (1943).
[23] O. Kratky and G. Porod, Rec. Trav. Chim. **68**, 1106 (1949).
[24] M. Doi and S. F. Edwards, *The Theory of Polymer Dynamics* (Oxford University Press, Oxford, 1989).
[25] A. Ahsan, J. Rudnick, and R. Bruinsma, Biophys. J. **74**, 132 (1998).
[26] J. F. Marko and E. D. Siggia, Biophys. J. **73**, 2173 (1997).
[27] J. Rudnick and R. Bruinsma, Biophys. J. **76**, 1725 (1999).
[28] M. Rief, J. M. Fernandez, and H. E. Gaub, Phys. Rev. Lett. **81**, 4764 (1998).
[29] D. K. Klimov and D. Thirumalai, Proc. Natl. Acad. Sci. U.S.A. **96**, 6166 (1999).
[30] A. Halperin and E. B. Zhulina, Europhys. Lett. **15**, 417 (1991).
[31] M. N. Tamashiro and H. Schiessel, Macromolecules **33**, 5263 (2000).
[32] T. A. Vilgis, A. Johner, and J.-F. Joanny, Eur. Phys. J. E **2**, 289 (2000).
[33] T. Soddemann, H. Schiessel, and A. Blumen, Phys. Rev. E **57**, 2081 (1998).
[34] H. Schiessel, W. M. Gelbart, and R. Bruinsma (unpublished).
[35] O. V. Borisov and A. Halperin, Macromolecules **29**, 2612 (1996); Europhys. Lett. **34**, 657 (1996); Macromolecules **30**, 4432 (1997); Phys. Rev. E **57**, 812 (1998); Eur. Phys. J. B **9**, 251 (1999).
[36] A. Buhot and A. Halperin, Phys. Rev. Lett. **84**, 2160 (2000).
[37] T. M. Birshtein and O. B. Ptitsyn, *Conformations of Macromolecules* (Wiley, New York, 1966).
[38] D. Poland and H. A. Scheraga, *Theory of Helix-Coil Transitions in Biopolymers* (Academic, New York, 1970).
[39] C. R. Cantor and P. R. Schimmel, *Biophysical Chemistry* (Freeman, San Francisco, 1980), Part III, Chap. 20.
[40] V. A. Bloomfield, Am. J. Phys. **67**, 1212 (1999).
[41] L. G. Presta and G. D. Rose, Science **240**, 1632 (1988).
[42] L. Regan and W. F. DeGrado, Science **241**, 976 (1988).
[43] M. Blaber, X. J. Zhang, and B. W. Matthews, Science **260**, 1637 (1993); **262**, 917 (1993).
[44] T. J. Deming, Nature (London) **390**, 386 (1997).
[45] B. H. Zimm and J. K. Bragg, J. Chem. Phys. **31**, 526 (1959).
[46] L. D. Landau and E. M. Lifshitz, *Statistical Physics* (Pergamon, Oxford, 1980).
[47] G. A. Carri and M. Muthukumar, Phys. Rev. Lett. **82**, 5405 (1999).
[48] U. H. E. Hansmann and Y. Okamoto, J. Chem. Phys. **110**, 1267 (1999); **111**, 1339 (1999).
[49] N. A. Alves and U. H. E. Hansmann, Phys. Rev. Lett. **84**, 1836 (2000).
[50] K. Nagai, J. Chem. Phys. **34**, 887 (1961).
[51] P. J. Flory, Science **124**, 53 (1956).
[52] R. M. Corless, G. H. Gonnet, D. E. G. Hare, D. J. Jeffrey, and D. E. Knuth, Adv. Comput. Math **5**, 329 (1996).
[53] J. P. Boyd, Appl. Math. Lett. **11** (6), 27 (1998).
[54] L. Lewin, *Polylogarithms and Associated Functions* (North-Holland, New York, 1981).